L. J. Gray

T. Kaplan

Computer Science and Mathematics Division,
Oak Ridge National Laboratory,
P.O. Box 2008, Building 6012,
Oak Ridge, TN 37831-6367

J. D. Richardson
Department of Mechanical Engineering,
Tennessee Technological University,
P.O. Box 5014,
Cookeville, TN 38505

G. H. Paulino[1]
Department of Civil and Environmental
Engineering,
University of Illinois at Urbana-Champaign,
Newmark Laboratory,
205 North Mathews Avenue,
Urbana, IL 61801
e-mail: paulino@uiuc.edu
Mem. ASME

Green's Functions and Boundary Integral Analysis for Exponentially Graded Materials: Heat Conduction

Free space Green's functions are derived for graded materials in which the thermal conductivity varies exponentially in one coordinate. Closed-form expressions are obtained for the steady-state diffusion equation, in two and three dimensions. The corresponding boundary integral equation formulations for these problems are derived, and the three-dimensional case is solved numerically using a Galerkin approximation. The results of test calculations are in excellent agreement with exact solutions and finite element simulations. [DOI: 10.1115/1.1485753]

1 Introduction

Functionally graded materials (FGMs) are an important area of materials science research, with potentially many important applications, e.g., super-heat resistance materials for thermal barrier coatings and furnace liners, vehicle and personal body armor, electromagnetic sensors, and graded refractive index materials for optical applications. In an ideal FGM, the material properties may vary smoothly in one dimension (e.g., are constant in (x, y) but vary with z). As an example, having a smooth transition region between a pure metal and pure ceramic would result in a material that combines the desirable high temperature properties and thermal resistance of a ceramic, with the fracture toughness of a metal. Comprehensive reviews of current FGM research may be found in the articles by Hirai [1], Markworth et al. [2] and Paulino et al. [3], and the book by Suresh and Mortensen [4].

Computational analysis can be an effective method for designing specific FGM systems, and for understanding FGM behavior. For homogeneous media, boundary integral equation methods (e.g., [5]) have been used extensively. However, the reformulation in terms of integral equations relies upon having, as either a closed form or a computable expression, a fundamental solution (Green's function) of the partial differential equation. Application of the boundary integral technique has therefore been limited, almost exclusively, to homogeneous, or piecewise homogeneous, media.

The fundamental solutions traditionally employed in boundary integral analysis for homogeneous materials are ''free space'' Green's functions: They satisfy the appropriate differential equation everywhere in space, except at the site where a point load

driving force is applied. Derivations for some of the basic Green's functions can be found in [5,6]. There has also been work in the direction of deriving Green's functions for a general nonhomogeneous material ([7–11]). Steady-state heat conduction with an arbitrary spatially varying conductivity has recently been investigated ([12,13]) and has generated some debate in the literature ([14,15]). In most cases, exact Green's functions are only obtained under certain restrictions.

In the present paper, we derive free space fundamental solutions for both the two-dimensional and three-dimensional FGM Laplace equation, assuming that the thermal conductivity varies exponentially. The corresponding boundary integral equation formulation, which turns out to be somewhat different from the homogeneous media case, is also obtained, and numerical results based upon a Galerkin approximation are presented. Relatively little attention has been paid to obtaining Green's functions for the special case of graded materials: A Green's function for a special type of elastodynamics problem was obtained by Vrettos [16], and exponential grading was also considered in [11]. The two-dimensional Green's function results have appeared in conjunction with a convective heat transfer problem in a *homogeneous* material ([17,18]), and moreover [19] essentially contains the Green's functions derived herein (obtained in a different manner). However, the analysis employed in this paper for heat conduction in an exponential FGM will carry over to the important case of elasticity ([20]), and thus it is deemed useful to present this alternate derivation in detail.

This paper is organized as follows. The three-dimensional Laplace equation is treated in Section 2.1, and the two-dimensional case in Section 2.2. Section 3 discusses some test results from a Galerkin numerical implementation of the boundary integral formulation, and Section 4 contains some concluding remarks. Finally, in the Appendix it is shown that the integral equations and Green's functions can be suitably modified to allow for a Symmetric-Galerkin implementation. Complete formulas for the three-dimensional reformulated fundamental solutions and their first and second derivatives, for the case that the thermal conductivity is real, are also given in this Appendix.

2 Green's Functions

Steady-state isotropic heat conduction in a solid is governed by the equation

$$\nabla \cdot (k \nabla \phi) = 0. \tag{1}$$

Here $\phi = \phi(x,y,z)$ is the temperature function, and we assume the functionally graded material is defined by the thermal conductivity

$$k(x,y,z) = k(z) = k_0 e^{-2i\alpha z}, \tag{2}$$

where α is real. This assumption of a purely imaginary exponent is apparently necessary for the derivation that follows. However, once the solution is obtained, it is readily seen to be valid for any complex α. Substituting Eq. (2) into Eq. (1), one obtains that the temperature satisfies

$$\nabla^2 \phi - 2i\alpha \phi_z = 0, \tag{3}$$

where ϕ_z denotes the derivative with respect to z.

The Green's function equation can be derived by constructing the integral equation corresponding to Eq. (3). Following the standard procedure, Eq. (3) is multiplied by an arbitrary function $f(x,y,z) = f(Q)$ and integrated over a bounded volume V. Integrating by parts, and denoting the boundary of V by Σ, one obtains

$$0 = \int_V f(Q)(\nabla^2 \phi(Q) - 2i\alpha \phi_z(Q))dV_Q.$$

$$= \int_\Sigma \left\{ f(Q) \frac{\partial}{\partial n} \phi(Q) - \phi(Q) \frac{\partial}{\partial n} f(Q) \right.$$

$$\left. - 2i\alpha n_z(Q)\phi(Q)f(Q) \right\} dQ + \int_V \phi(Q)(\nabla^2 f(Q)$$

$$+ 2i\alpha f_z(Q))dV_Q, \tag{4}$$

where $\mathbf{n}(Q) = (n_x, n_y, n_z)$ is the unit outward normal for Σ. If $f(Q) = G(P,Q)$ satisfies the Green's function equation (the adjoint to Eq. (3))

$$\nabla^2 G(P,Q) + 2i\alpha G_z(P,Q) = -\delta(Q-P), \tag{5}$$

where δ is the Dirac delta function, the remaining volume integral becomes simply $-\phi(P)$. Thus we obtain the governing boundary integral equation

$$\phi(P) + \int_\Sigma \phi(Q)\left(\frac{\partial}{\partial n} G(P,Q) + 2i\alpha n_z G(P,Q) \right) dQ$$

$$= \int_\Sigma G(P,Q) \frac{\partial}{\partial n} \phi(Q)dQ, \tag{6}$$

which differs in form from the usual integral statements by the presence of the additional term multiplying $\phi(Q)$. With obvious changes (e.g., line integrals instead of surface integrals), the above equations are equally valid for two dimensions. We first derive the Green's function for three dimensions.

2.1 Three Dimensions. Let $\hat{f}(\boldsymbol{\omega})$ denote the Fourier transform of a function $\mathcal{F}(Q)$,

$$\hat{f}(\boldsymbol{\omega}) = \int_{\mathcal{R}^3} \mathcal{F}(Q)e^{-i\boldsymbol{\omega}\cdot Q}dQ \tag{7}$$

where $\boldsymbol{\omega} = (\omega_x, \omega_y, \omega_z)$ is the transform variable and the dot represents the inner product. Transforming Eq. (5) and solving for $\hat{G}(\boldsymbol{\omega})$ (the transform of G with respect to Q), yields

$$\hat{G}(\boldsymbol{\omega}) = \frac{e^{-i\boldsymbol{\omega}\cdot P}}{\omega^2 + 2\alpha\omega_z}, \tag{8}$$
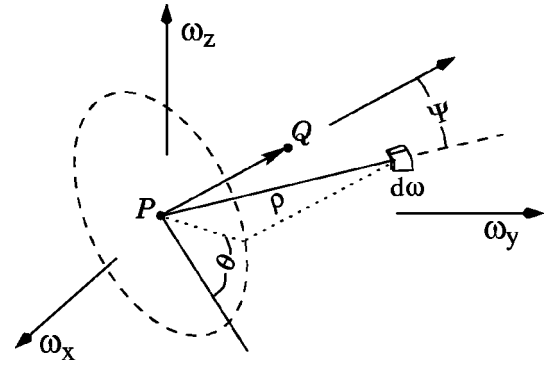

Fig. 1 Spherical coordinate system for evaluating the ω integral

where $\omega^2 = \boldsymbol{\omega}\cdot\boldsymbol{\omega}$. Applying the inverse transform, one obtains

$$G(P,Q) = \frac{1}{(2\pi)^3} \int_{\mathcal{R}^3} \frac{e^{i\boldsymbol{\omega}\cdot(Q-P)}}{\omega^2 + 2\alpha\omega_z} dw, \tag{9}$$

where dw is shorthand for the three-dimensional differential element, i.e., $dw = d\omega_x d\omega_y d\omega_z$. Changing variables

$$\omega_z \rightarrow \omega_z - \alpha \tag{10}$$

and setting $R = Q - P$, $R_z = Q_z - P_z$, we obtain

$$G(P,Q) = \frac{1}{(2\pi)^3} e^{-i\alpha R_z} \int_{\mathcal{R}^3} \frac{e^{i\boldsymbol{\omega}\cdot R}}{\omega^2 - \alpha^2} d\omega, \tag{11}$$

which can be conveniently split into two terms,

$$G(P,Q) = \frac{e^{-i\alpha R_z}}{(2\pi)^3} \left[\int_{\mathcal{R}^3} \frac{e^{i\boldsymbol{\omega}\cdot R}}{\omega^2} d\omega + \alpha^2 \int_{\mathcal{R}^3} \frac{e^{i\boldsymbol{\omega}\cdot R}}{\omega^2(\omega^2 - \alpha^2)} d\omega \right]. \tag{12}$$

The first integral is Eq. (9) with $\alpha = 0$, and is therefore recognized as the Green's function for the Laplace equation (constant k), the point source potential:

$$\frac{e^{-i\alpha R_z}}{(2\pi)^3} \int_{\mathcal{R}^3} \frac{e^{i\boldsymbol{\omega}\cdot R}}{\omega^2} d\omega = \frac{e^{-i\alpha R_z}}{4\pi r}, \tag{13}$$

where $r = \|R\| = \|Q - P\|$ is the distance between the source point P and the field point Q.

To evaluate the second term in Eq. (12), it is convenient to employ spherical coordinates (ρ, θ, ψ), with, however, the axis defining the pole $\psi = 0$ taken as the direction R/r instead of the z-axis (see Fig. 1). The integration limits are $0 < \rho < \infty$, $0 \leq \psi \leq \pi$, and $0 \leq \theta \leq 2\pi$; however, for the residue calculations to follow, it will be much more convenient to have $-\infty < \rho < \infty$ and $0 \leq \psi \leq \pi/2$. With the standard limits, the residue calculation must shift half-planes depending upon the sign of $\cos(\psi)$; more importantly, starting at $\rho = 0$ would force consideration of contours along the imaginary axis, necessary to work with the imaginary part of the exponential. In comparison, if ρ varies over the entire real axis, a simple semicircle in the upper half-plane suffices. To this end, if the function f satisfies $f(\rho, \psi) = f(-\rho, \pi - \psi)$, then

$$\int_0^\infty \int_0^\pi f(\rho, \psi)d\psi d\rho$$

$$= \int_0^\infty \int_0^{\pi/2} f(\rho, \psi)d\psi d\rho + \int_0^\infty \int_{\pi/2}^\pi f(\rho, \psi)d\psi d\rho$$

$$= \int_0^\infty \int_0^{\pi/2} f(\rho, \psi)d\psi d\rho + \int_0^\infty \int_0^{\pi/2} f(\rho, \pi - \psi)d\psi d\rho$$
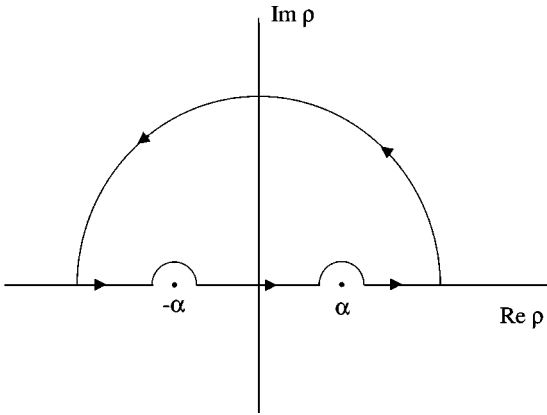
Fig. 2 Contour in the complex plane used to compute the ρ integration

$$= \int_0^\infty \int_0^{\pi/2} f(\rho,\psi) d\psi d\rho + \int_{-\infty}^0 \int_0^{\pi/2} f(-\rho,\pi-\psi) d\psi d\rho$$

$$= \int_{-\infty}^\infty \int_0^{\pi/2} f(\rho,\psi) d\psi d\rho. \tag{14}$$

It will turn out that the function to be integrated satisfies the above constraint, and thus the modified limits of integration for ρ and ψ can be employed. As mentioned above, this greatly simplifies the residue procedures for the ρ integration.

Noting that $\boldsymbol{\omega}\cdot\mathbf{R} = \rho r \cos(\psi)$ and that, other than this exponential, the integrand is a function of ω^2 and independent of θ, this second term therefore becomes

$$\frac{\alpha^2 e^{-i\alpha R_z}}{(2\pi)^2} \int_0^{\pi/2} \sin(\psi) d\psi \int_{-\infty}^\infty \frac{e^{i\rho r \cos(\psi)}}{\rho^2 - \alpha^2} d\rho. \tag{15}$$

Using the contour shown in Fig. 2, the ρ integration is a straightforward exercise in residue calculus, yielding

$$\int_{-\infty}^\infty \frac{e^{i\rho r \cos(\psi)}}{\rho^2 - \alpha^2} d\rho = -\frac{\pi}{\alpha} \sin(\alpha r \cos(\psi)). \tag{16}$$

The final integration,

$$-\frac{\pi}{\alpha} \int_0^{\pi/2} \sin(\psi)\sin(\alpha r \cos(\psi)) d\psi, \tag{17}$$

follows from a simple change of variables, and thus the second term is seen to be

$$\frac{e^{-i\alpha R_z}\cos(\alpha r)}{4\pi r} - \frac{e^{-i\alpha R_z}}{4\pi r}. \tag{18}$$

Including Eq. (13), we find the simple result

$$G(P,Q) = \frac{e^{-i\alpha R_z}\cos(\alpha r)}{4\pi r}. \tag{19}$$

Although this result was derived assuming that α is real, it is a simple matter to check by direct calculation that Eq. (19) satisfies Eq. (5) for any complex α. It is useful, especially for the discussion of the two-dimensional case that follows, to observe that

$$G(P,Q) = e^{-i\alpha R_z}\frac{e^{-i\alpha r}}{4\pi r} \tag{20}$$

is an equally valid solution of Eq. (5) for α real. Moreover, the added $\sin(\alpha r)/r$ term is regular as $r\to 0$, and thus does not alter the delta function at $Q=P$. Replacing α by $i\beta_0$, where β_0 is real, we obtain

$$G(P,Q) = \frac{e^{\beta_0(r+R_z)}}{4\pi r} \tag{21}$$

as the Green's function for $k(z) = e^{2\beta_0 z}$.

In the derivation of the boundary integral equation, a sphere S_ε of radius ε centered at the interior point P would be removed from V, and the integration over Σ would include the surface of this sphere. The limit as $\varepsilon\to 0$ of the integral

$$\int_{S_\varepsilon}\left\{ G(P,Q)\frac{\partial}{\partial n}\phi(Q) - \phi(Q)\frac{\partial}{\partial n}G(P,Q) \right.$$

$$\left. -2i\alpha(\phi(Q)G(P,Q))n_z \right\} dQ \tag{22}$$

must therefore be considered. However, for $r\to 0$,

$$\frac{\partial}{\partial n}G(P,Q) \approx \frac{\partial}{\partial n}\frac{1}{4\pi r} \tag{23}$$

and the $\varepsilon = 0$ limit does indeed produce the correct value $-\phi(P)$.

Finally, it is useful to note that Eq. (18) can, from the point of view of the singularity at $r=0$, be considered as a remainder term. That is, the singularity for the FGM Green's function is entirely contained within Eq. (13), the homogeneous steady-state solution, as Eq. (18) is regular at $r=0$.

2.2 Two Dimensions. The Green's function $g(x_Q,z_Q;x_P,z_P)$ for the two-dimensional equation,

$$\phi_{xx} + \phi_{zz} - 2i\alpha\phi_z = 0, \tag{24}$$

is expected to behave as $\log(r)$, and as this function does not die off at infinity, the above Fourier transform approach is doomed to fail. However, this fundamental solution can be viewed as the response seen at the point $(x_Q,0,z_Q)$ to a uniform distribution of charge along the y-axis. This response should be the result of integrating the three-dimensional Green's function over this axis, which for the homogeneous case takes the form

$$\frac{1}{4\pi} \int_{-\infty}^\infty \frac{dy_P}{((x_Q-x_P)^2 + y_P^2 + (z_Q-z_P)^2)^{1/2}}. \tag{25}$$

The fact that the integral doesn't exist is a minor inconvenience that is remedied by doing the analysis for $\partial G/\partial x_Q$ ([21]). The integral of this function with respect to y_P does exist, and followed by an integration over x_Q, the correct $\log(r)$ result is obtained, where r is now the two-dimensional distance.

With this framework in mind, we observe that the three-dimensional functionally graded material (FGM) Green's function, in the form of Eq. (20), is $e^{-i\alpha R_z}$ times the fundamental solution for the Helmholtz Eq. (3). Since this prefactor is independent of y_P, integrating out this coordinate as in Eq. (25), we expect that the two-dimensional FGM Green's function is given by

$$g(x_Q,z_Q;x_P,z_P) = \frac{i}{4}e^{-i\alpha R_z}H_0^1(\alpha r). \tag{26}$$

Here, H_0^1 is the zeroth-order first kind Hankel function ([22]), well known to be the solution of the Helmholtz equation in two dimensions. This expectation can be established simply by differentiating Eq. (26) and checking that

$$g_{xx} + g_{zz} + 2i\alpha g_z = 0, \tag{27}$$

for $Q\neq P$ (this is the two-dimensional analogue of the Green's function equation, Eq. (5)). That this differentiation also yields a delta function at $Q=P$ follows from the known behavior of H_0^1 for the Helmholtz equation. Finally, it should be noted that the two-dimensional boundary integral equation becomes

$$\phi(P) + \int_{\Sigma} \phi(Q) \left(\frac{\partial}{\partial n} g(P,Q) + 2i\alpha n_z g(P,Q) \right) dQ$$

$$= \int_{\Sigma} g(P,Q) \frac{\partial}{\partial n} \phi(Q) dQ, \qquad (28)$$

which corresponds to Eq. (6) with $G(P,Q)$ (three-dimensional case) replaced by $g(P,Q)$ (two-dimensional case).

2.3 Extensions. As it may be useful to have the material properties vary in more than one component ([23]), it is worth noting that the above analysis extends to a more general exponential variation for k,

$$k(x,y,z) = k_0 e^{-2i\boldsymbol{\alpha}\cdot Q}, \qquad (29)$$

where $\boldsymbol{\alpha} = (\alpha_x, \alpha_y, \alpha_z)$. The three-dimensional Green's function is now given by

$$G_{xyz}(P,Q) = \frac{e^{-i\boldsymbol{\alpha}\cdot R} \cos((\boldsymbol{\alpha}\cdot\boldsymbol{\alpha})r)}{4\pi r}. \qquad (30)$$

Comparing this with Eq. (19), it is not surprising that the two-dimensional result in this case (again dropping out the y-coordinate) becomes

$$g_{xz}(x_Q, z_Q; x_P, z_P) = \frac{i}{4} e^{-i\boldsymbol{\alpha}\cdot R} H_0^1((\boldsymbol{\alpha}\cdot\boldsymbol{\alpha})r). \qquad (31)$$

2.4 Galerkin Approximation. The numerical results presented in the next section utilize the Galerkin approximation ([5]) to reduce the integral equation to a finite system of equations. Here we briefly review this technique, starting by rewriting Eq. (6) as

$$\mathcal{P}(P) \equiv \phi(P) + \int_{\Sigma} \phi(Q) \left(\frac{\partial}{\partial n} G(P,Q) + 2i\alpha n_z G(P,Q) \right) dQ$$

$$- \int_{\Sigma} G(P,Q) \frac{\partial}{\partial n} \phi(Q) dQ = 0. \qquad (32)$$

As is usual, basis shape functions $\psi_j(Q)$ are used to interpolate the boundary from the element nodal coordinates, and to approximate the surface potential and flux in terms of nodal values, i.e.,

$$\Sigma(\eta, \xi) = \sum_j (x_j, y_j, z_j) \psi_j(\eta, \xi)$$

$$\phi(Q) = \sum_j \phi_j \psi_j(Q) \qquad (33)$$

$$\frac{\partial \phi}{\partial n}(Q) = \sum_j \left(\frac{\partial \phi}{\partial n} \right)_j \psi_j(Q).$$

The numerical results reported herein employ a six-noded quadratic triangular element, defined using the right triangle parameter space (η, ξ), $\eta \geq 0$, $\xi \geq 0$, $\eta + \xi \leq 1$. The shape functions are given by

$$\psi_1(\eta, \xi) = (1 - \eta - \xi)(1 - 2\eta - 2\xi) \quad \psi_4(\eta, \xi) = 4\eta(1 - \eta - \xi)$$

$$\psi_2(\eta, \xi) = \eta(2\eta - 1) \qquad\qquad \psi_5(\eta, \xi) = 4\eta\xi \qquad (34)$$

$$\psi_3(\eta, \xi) = \xi(2\xi - 1) \qquad\qquad \psi_6(\eta, \xi) = 4\xi(1 - \eta - \xi).$$

In a Galerkin approximation, these shape functions are employed as weighting functions for enforcing Eq. (32) "on average," i.e.,

$$\int_{\Sigma} \psi_k(P) \int_{\Sigma} \mathcal{P}(P) dP = 0. \qquad (35)$$

When the approximations in Eq. (33) are incorporated into this equation, the resulting finite system of equations can be discretized and solved numerically.

It should also be noted that, unlike the Green's function $1/(4\pi r)$ for the Laplace equation (homogeneous problem), neither Eq. (20) nor Eq. (26) is a symmetric function of P and Q. It would therefore appear impossible to have a symmetric-Galerkin approximation ([24–28]), as this formulation demands a symmetric Green's function. However, as shown in the Appendix, a slight reworking of the equations and the kernel functions restores all of the necessary symmetry properties. This Appendix also provides formulas for all of the kernel functions: temperature and flux equations in two and three dimensions.

3 Numerical Examples

The three-dimensional steady-state fundamental solution has been incorporated into a boundary element method (BEM) algorithm. As noted above, the integral Eq. (6) is numerically approximated via the (nonsymmetric) Galerkin method (see Eq. (35)), together with standard six-node isoparametric quadratic triangular elements to interpolate the boundary and boundary functions. For the numerical examples, the conservation Eq. (1) will be taken as energy conservation in a functionally graded media under the condition of steady-state heat conduction without volumetric generation. To validate the numerical implementation, solutions to two test problems are presented below: In the first, the domain is a simple cube and the exact solution is known; the second involves a curved geometry which may be more representative of an actual systems component.

3.1 Unit Cube: Linear Heat Flux. For the first example problem, the geometry is a unit cube with the origin of a Cartesian system fixed at one corner. The thermal conductivity in this example is taken to be

$$k(z) = k_0 e^{2\beta z} = 5e^{3z}. \qquad (36)$$

The cube is insulated on the faces $[y=0]$ and $[y=1]$, while uniform heat fluxes of 5000 [POWER/AREA] are added and removed, respectively, at the $[x=1]$ and $[x=0]$ faces. In addition, the $[z=0]$ face is specified to have an x-dependent temperature distribution $T = 1000 x$ deg and at $[z=1]$ a normal heat flux of $q = 15000 x$ is removed. The analytic solution for this problem is

$$T = 1000xe^{-3z}$$

$$\mathbf{q} = -5000\hat{\mathbf{i}} + 15000x\hat{\mathbf{k}} \qquad (37)$$

where $\hat{\mathbf{i}}$ is a unit vector in the x-direction.

The results of the numerical simulations for the temperature distributions along an edge are shown in Fig. 3. The plot also includes the results obtained from a finite element method (FEM) simulation using a commercial package. In the FEM simulation,
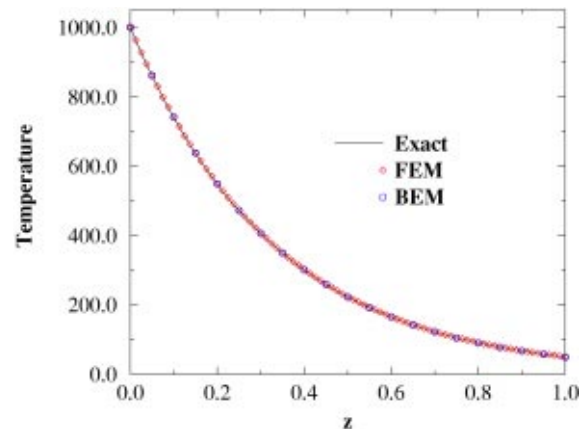

Fig. 3 Temperature distribution in the functionally graded material (FGM) unit cube along the edge $[x=1, y=1]$
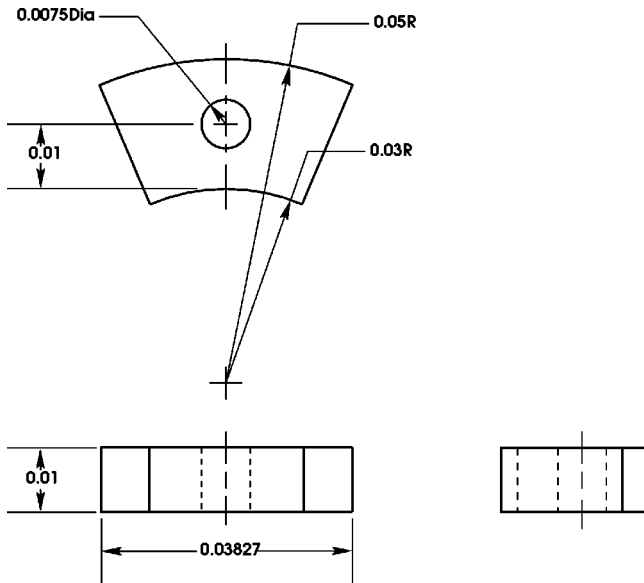
Fig. 4 Geometry of the functionally graded rotor

Fig. 6 Thermal conductivity profiles for the computational models of the rotor

40 homogeneous layers were used to approximate the continuous grading; the conductivity of each layer was computed from Eq. (36) where z was taken as the z-coordinate of the layer's centroid. The FEM elements used were 20-node quadratic brick elements and each of the 40 layers contained 400 brick elements, resulting in a total of 69,720 nodes. In the boundary element method (BEM) solution, a uniform grid consisting of isosceles right triangles, with each leg having length 0.1, was employed, resulting in a total of 1200 elements and 2646 nodes.

3.2 Functionally Graded Material (FGM) Rotor. The second numerical example is a rotor with eight mounting holes. Due to the eightfold symmetry, only one-eighth of the rotor is modeled, as drawn in Fig. 4. The grading direction for the rotor is parallel to its line of symmetry, which is taken as the z-axis, and the thermal conductivity for the rotor varies according to

$$\mathrm{k}(z) = 20 e^{330z} \frac{\mathrm{W}}{\mathrm{m\,K}}. \qquad (38)$$

A schematic for the thermal boundary conditions is shown in Fig. 5. The temperature is specified along the inner and outer radii and a uniform heat flux of 5×10^5 W/m^2 is added on the bottom surface where $z = 0$. All other surfaces are insulated as shown.

The BEM solution is compared with an FEM solution obtained from the same package used in the previous example using ten-
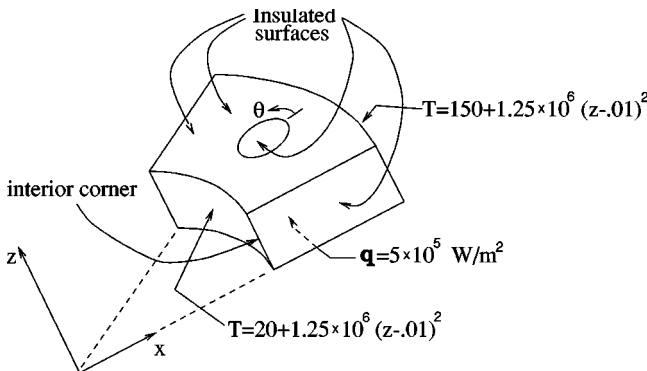

Fig. 7 Surface mesh employed on the functionally graded rotor
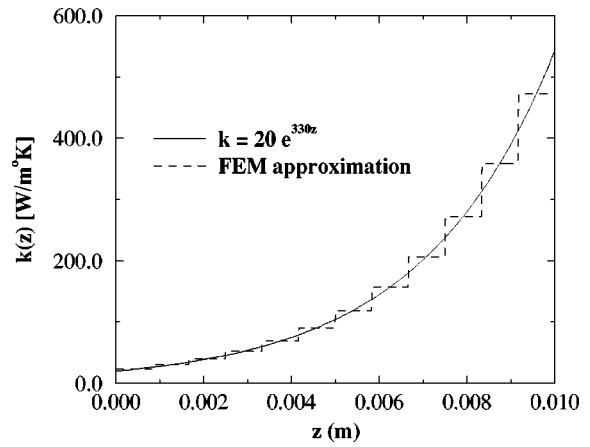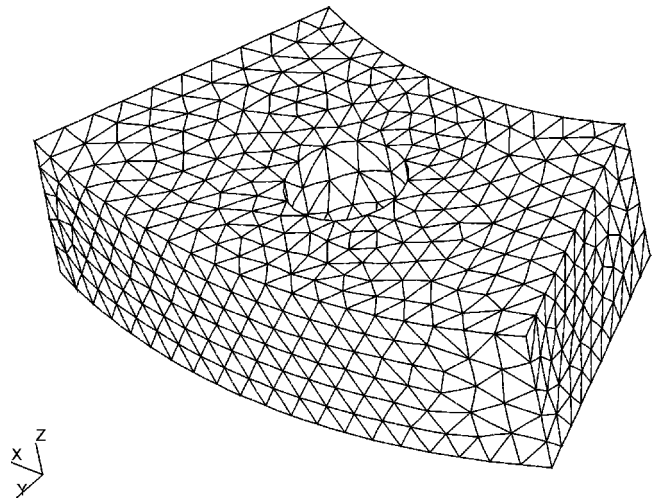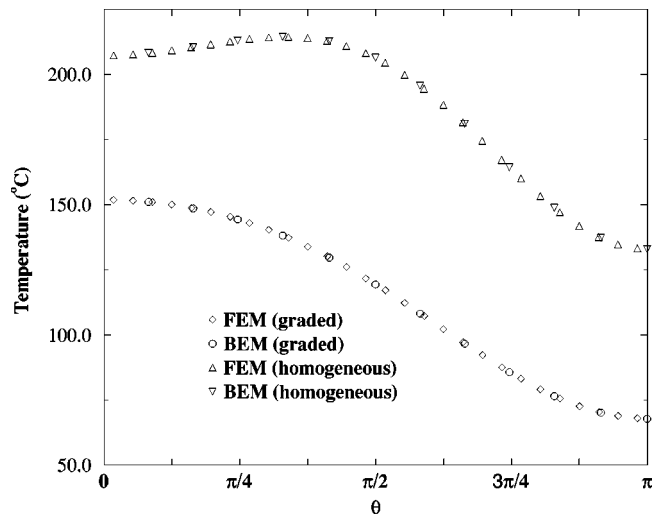

Fig. 8 Temperature distribution around the hole on the $z = 0.01$ surface

Fig. 5 Thermal boundary conditions on the rotor

node tetrahedral elements to handle the geometric complexity of the rotor. Due to resource limitations, the FEM model was limited to 12 layers which resulted in the rather crude conductivity profile shown in Fig. 6. Even so, the FEM mesh required 95,880 nodes,
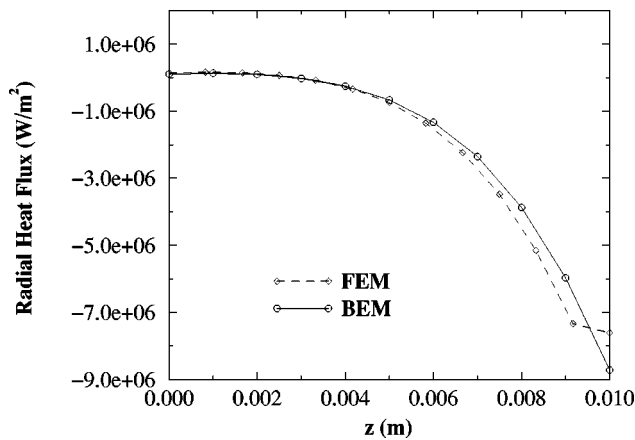
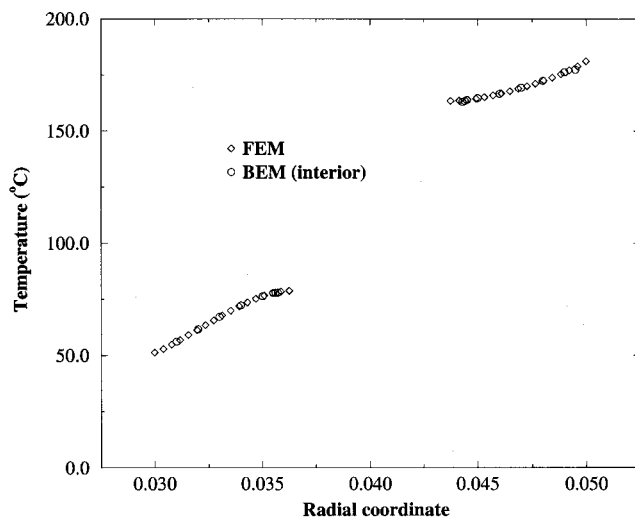**Fig. 9 Radial heat flux along the inside corner**

Fig. 10 Computed interior temperature values in the graded rotor

whereas the BEM mesh employed 3252. The mesh employed for the boundary integral analysis is shown in Fig. 7.

The temperature distribution around the hole is shown in Fig. 8. The angle θ is measured from a line passing through the line of symmetry for the geometry and the center line of the hole. Though surface nodal positions in the two models were not coincident in general, the plot shows a strong agreement in the two solutions. To see the effects of the grading upon the solution, the corresponding results for the *ungraded* rotor, $\beta=0$ ($k(z)\equiv20$), are also shown.

The radial heat flux along the line shown as the interior corner in Fig. 5 is plotted in Fig. 9. The negative sign indicates that the flow of heat is toward the interior of the rotor. A limitation on the use of piecewise constant conductivities in FEM models may be evident in the plot where the FEM nodal value at $z=0.01$ seems to fall out of line with the other values on the curve. The behavior should be fully expected, however, given the local error associated with the piecewise constant approximation seen near $z=0.01$ in Fig. 6. As should also be expected, the nodal flux values from the BEM solution seem to fall onto a single curve even in the region of the steepest conductivity gradient. This is *not* to say that BEM is necessarily better than FEM for graded analysis: The finite element method is not restricted to using the discontinuous piecewise constant approximation presently available in existing packages. It is possible to incorporate continuous grading within

individual elements, as demonstrated recently by Kim and Paulino [29] using a generalized isoparametric formulation.

As a final test, Fig. 10 displays a comparison between the FEM interior temperature values, and corresponding values computed from the BEM solution (in a post-processing calculation). The values are shown for a line of points on the mid-z ($z=0.005$) plane in the radial direction, passing through the middle of the hole. Again, the BEM and FEM results agree quite well.

4 Conclusions

The primary conclusion of this work is that boundary integral analysis, for the most part limited to applications involving homogeneous or piecewise homogeneous media, can be successfully applied to exponentially graded materials. Although the simplest case, namely the Laplace equation, has been treated herein, it is expected that other applications, including transient diffusion ([30]) and elasticity ([20]), can also be addressed. Note that a specific elastodynamics problem has already been addressed by Vrettos [16].

The numerical results presented in this paper have shown that it is simple to implement the functionally graded material (FGM) Green's function in a standard boundary integral (Galerkin) approximation, and that accurate results are obtained. For graded materials, this offers the possibility of efficient and accurate solution of those types of problems for which a boundary integral analysis is particularly advantageous, such as shape optimization, moving boundaries, and small-scale structures.

Appendix

Symmetric Kernels. The symmetric-Galerkin method ([25–28]) is a highly effective numerical technique for boundary integral analysis. As the name implies, it utilizes the Galerkin approximation to induce a symmetric coefficient matrix. The symmetry comes about because of the symmetry properties of the kernel functions in the integral equations for surface temperature and for surface flux. Note that for the homogeneous Laplace equation, the fundamental solution is symmetric, $G(P,Q)=G(Q,P)$, but the functionally graded material (FGM) Green's function, Eq. (21), is not. Thus it would appear that a symmetric-Galerkin approximation is not possible.

In this section, the FGM boundary integral equations are reformulated to allow a symmetric numerical implementation. In addition, formulas for all of the required FGM kernel functions for $k(z)$ real,

$$k(z)=k_0 e^{2\beta_0 z}, \tag{39}$$

are conveniently summarized.

To obtain a symmetric matrix, the equations have to be written in terms of the surface flux,

$$\mathcal{F}(Q)=-k(z_Q)\frac{\partial}{\partial n}\phi(Q) \tag{40}$$

rather than the normal derivative. The equation for surface temperature $\phi(P)$ is therefore

$$\phi(P) + \int_\Sigma F(P,Q)\phi(Q)dQ = \int_\Sigma G_S(P,Q)\mathcal{F}(Q)dQ, \quad (41)$$

and in three dimensions the kernel functions are

$$G_S(P,Q) = -\frac{G(P,Q)}{\mathrm{k}(z_Q)} = -\frac{1}{4\mathrm{k}_0\pi}\frac{e^{\beta_0(r-z_Q-z_P)}}{r}$$

$$F(P,Q) = \frac{\partial}{\partial n}G(P,Q) - 2\beta_0 n_z G(P,Q)$$

$$= -\frac{e^{\beta_0(r+R_z)}}{4\pi}\left(\frac{\mathbf{n}\cdot R}{r^3} - \beta_0\frac{\mathbf{n}\cdot R}{r^2} + \beta_0\frac{n_z}{r}\right). \quad (42)$$

Most importantly, note that $G_S(P,Q)$, unlike G, is symmetric with respect to P and Q. This is the first of three conditions needed for symmetry. The other two conditions involve the flux equation. Differentiating Eq. (41) with respect to P, dotting with $\mathbf{N} = \mathbf{N}(P)$, and multiplying by $-\mathrm{k}(z_P)$ yields the corresponding equation for surface flux

$$\mathcal{F}(P) + \int_\Sigma W(P,Q)\phi(Q)dQ = \int_\Sigma S(P,Q)\mathcal{F}(Q)dQ. \quad (43)$$

The kernel functions, again for three dimensions, are computed to be

$$S(P,Q) = -\mathrm{k}(z_P)\frac{\partial}{\partial N}G_S(P,Q)$$

$$= -\frac{e^{\beta_0(r-R_z)}}{4\pi}\left(-\frac{\mathbf{N}\cdot R}{r^3} + \beta_0\frac{\mathbf{N}\cdot R}{r^2} + \beta_0\frac{N_z}{r}\right). \quad (44)$$

and

$$W(P,Q) = -\mathrm{k}(z_P)\frac{\partial}{\partial N}F(P,Q) = \frac{\mathrm{k}_0}{4\pi}e^{\beta_0(r+z_Q+z_P)}$$

$$\times\left(3\frac{(\mathbf{n}\cdot R)(\mathbf{N}\cdot R)}{r^5} - 3\beta_0\frac{(\mathbf{n}\cdot R)(\mathbf{N}\cdot R)}{r^4}\right.$$

$$+ \frac{\beta_0^2(\mathbf{n}\cdot R)(\mathbf{N}\cdot R) - \beta_0(N_z\mathbf{n} - n_z\mathbf{N})\cdot R - \mathbf{n}\cdot\mathbf{N}}{r^3}$$

$$\left.+ \beta_0\frac{\beta_0(N_z\mathbf{n} - n_z\mathbf{N})\cdot R + \mathbf{n}\cdot\mathbf{N}}{r^2} - \beta_0^2\frac{N_z n_z}{r}\right). \quad (45)$$

The additional symmetry requirements are that W must be symmetric, $W(P,Q) = W(Q,P)$, and that $S(P,Q) = F(Q,P)$. Interchanging Q and P implies replacing $\mathbf{N}(P)$ with $\mathbf{n}(Q)$ and changes the sign of R, and thus both conditions are seen to hold.

References

[1] Hirai, T., 1996, ''Functionally Graded Materials,'' *Materials Science and Technology*, R. J. Brook, ed., Vol. 17B of *Processing of Ceramics*, Part 2, VCH Verlagsgesellschaft mbH, Weinheim, Germany, pp. 292–341.
[2] Markworth, A. J., Ramesh, K. S., and Parks, W. P. Jr., 1995, ''Modelling Studies Applied to Functionally Graded Materials,'' J. Mater. Sci., **30**, pp. 2183–2193.
[3] Paulino, G. H., Jin, Z.-H., and Dodds, R. H., 2003, ''Failure of Functionally Graded Materials,'' *Comprehensive Structural Integrity*, B. Karihaloo, R. Ritchie and I. Milne, eds., **2**, Elsevier, New York, Chap. 13.
[4] Suresh, S., and Mortensen, A., 1998, *Fundamentals of Functionally Graded Materials*, The Institute of Materials, IOM Communications Ltd., London.
[5] Bonnet, M., 1995, *Boundary Integral Equation Methods for Solids and Fluids*, John Wiley and Sons, New York.
[6] Barton, G., 1999, *Elements of Green's Functions and Propagation*, Oxford University Press, Oxford, UK.
[7] Ang, W. T., Kusuma, J., and Clements, D. L., 1996, ''A Boundary Element Method for a Second Order Elliptic Partial Differential Equation With Variable Coefficients,'' Eng. Anal. Boundary Elem., **18**, pp. 311–316.
[8] Clements, D. L., 1980, ''A Boundary Integral Equation Method for the Numerical Solution of a Second Order Elliptic Equation With Variable Coefficients,'' J. Aust. Math. Soc. B, Appl. Math., **22**, pp. 218–228.
[9] Shaw, R. P., 1994, ''Green's Functions for Heterogeneous Media Potential Problems,'' Eng. Anal. Boundary Elem., **13**, pp. 219–221.
[10] Shaw, R. P., and Makris, N., 1992, ''Green's Functions for Helmholtz and Laplace Equations in Heterogeneous Media,'' Eng. Anal. Boundary Elem., **10**, pp. 179–183.
[11] Shaw, R. P., and Manolis, G. D., 2000, ''A Generalized Helmholtz Equation Fundamental Solution Using a Conformal Mapping and Dependent Variable Transformation,'' Eng. Anal. Boundary Elem., **24**, pp. 177–188.
[12] Divo, E., and Kassab, A. J., 1998, ''Generalized Boundary Integral Equation for Heat Conduction in Non-homogeneous Media: Recent Developments on the Sifting Property,'' Eng. Anal. Boundary Elem., **22**, pp. 221–234.
[13] Kassab, A. J., and Divo, E., 1996, ''A Generalized Boundary Integral Equation for Isotropic Heat Conduction With Spatially Varying Thermal Conductivity,'' Eng. Anal. Boundary Elem., **18**, pp. 273–286.
[14] Bonnet, M., and Guiggiani, M., 1998, Comments about the paper entitled ''A Generalized Boundary Integral Equation for Isotropic Heat Conduction With Spatially Varying Thermal Conductivity,'' by A. J. Kassab and E. Divo, Eng. Anal. Boundary Elem., **22**, pp. 235–240.
[15] Power, H., 1997, ''On the Existence of Kassab and Divo's Generalized Boundary Integral Equation Formulation for Isotropic Heterogeneous Steady State Heat Conduction Problems,'' Eng. Anal. Boundary Elem., **20**, pp. 341–345.
[16] Vrettos, C., 1991, ''Surface Green's Functions for Continuously Nonhomogeneous Soil,'' *Computer Methods and Advances in Geomechanics*, Beer, Booker, and Carter, eds., Rotterdam, Balkema, pp. 801–804.
[17] Li, B. Q., and Evans, J. W., 1991, ''Boundary Element Solution of Heat Convection-Diffusion Problems,'' J. Comput. Phys., **93**, pp. 255–272.
[18] Wrobel, L. C., personal communication.
[19] Shaw, R. P., and Gipson, G. S., 1995, ''Interrelated Fundamental Solutions for Various Heterogeneous Potential, Wave and Advective-Diffusive Problems,'' Eng. Anal. Boundary Elem., **16**, pp. 29–34.
[20] Martin, P. A., Richardson, J. D., Gray, L. J., and Berger, J., 2002, ''On Green's Function for a Three-Dimensional Exponentially-Graded Elastic Solid,'' Proc. Royal Soc. London A, in press.
[21] Kellogg, O. D., 1953, *Foundations of Potential Theory*, Dover, New York.
[22] Olver, F. W. J., 1972, ''Bessel Functions of Integer Order,'' *Handbook of Mathematical Functions*, M. Abramowitz and I. A. Stegun, eds., National Bureau of Standards, Washington, D.C., Chap. 9, pp. 355–434.
[23] Konda, N., and Erdogan, F., 1994, ''The Mixed Mode Crack Problem in a Nonhomogeneous Elastic Medium,'' Eng. Fract. Mech., **47**, pp. 533–545.
[24] Bonnet, M., Maier, G., and Polizzotto, C., 1998, ''Symmetric Galerkin Boundary Element Method,'' ASME Appl. Mech. Rev., **51**, pp. 669–704.
[25] Hartmann, F., Katz, C., and Protopsaltis, B., 1985, ''Boundary Elements and Symmetry,'' Ing.-Arch., **55**, pp. 440–449.
[26] Maier, G., Diligenti, M., and Carini, A., 1991, ''A Variational Approach to Boundary Element Elastodynamic Analysis and Extension to Multidomain Problems,'' Comp. Meth. Appl. Eng., **92**, pp. 193–213.
[27] Sirtori, S., 1979, ''General Stress Analysis Method by Means of Integral Equations and Boundary Elements,'' Meccanica, **14**, pp. 210–218.
[28] Sirtori, S., Maier, G., Novati, G., and Miccoli, S., 1992, ''A Galerkin Symmetric Boundary Element Method in Elasticity: Formulation and Implementation,'' Int. J. Numer. Methods Eng., **35**, pp. 255–282.
[29] Kim, J.-H., and Paulino, G. H., 2002, ''Finite Element Evaluation of Mixed Mode Stress Intensity Factors in Functionally Graded Materials,'' Int. J. Numer. Methods Eng., **53**, pp. 1903–1935.
[30] Sutradhar, A., Paulino, G. H., and Gray, L. J., 2002, ''Transient Heat Conduction in Homogeneous and Non-homogeneous Materials by the Laplace Transform Galerkin Boundary Element Method,'' Eng. Anal. Boundary Elem., **26**, pp. 119–132.